Journal of Magnetic Resonance **151,** 284–290 (2001)
doi:10.1006/jmre.2001.2355, available online at http://www.idealibrary.com on IDEAL®

Angular Flow in Toroid Cavity Probes

Peter Trautner,* Klaus Woelk,*,[1] Joachim Bargon,* and Rex E. Gerald II†,[1]

*Institute of Physical and Theoretical Chemistry, University of Bonn, Wegelerstrasse 12, D-53115 Bonn, Germany; and †Chemical Technology Division, Argonne National Laboratory, 9700 South Cass Avenue, Argonne, Illinois 60439

E-mail: woelk@thch.uni-bonn.de; gerald@cmt.anl.gov

Received December 11, 2000; revised April 11, 2001; published online July 3, 2001

NMR signals from samples that rotate uniformly about the central conductor of a TCD (*t*oroid *c*avity *d*etector) exhibit frequency shifts that are directly proportional to the sample's angular velocity. This newly observed effect is based on the unique radiofrequency field inside TCDs, which is variable in direction. If a liquid sample is pumped through a capillary tube wound about the central conductor, the frequency shift is proportional to the flow rate. A mathematical relationship between a volumetric flow rate and the frequency shift is established and experimentally verified to high precision. Additionally, two-dimensional flow-resolved NMR spectroscopy for discrimination between components with different flow velocities yet retaining chemical shift information for structural analysis is presented. The application of the two-dimensional method in chromatographic NMR is suggested. Furthermore, utilization of the frequency-shift effect for rheologic studies if combined with toroid-cavity rotating-frame imaging is proposed.

Key Words: **toroid cavity detector; angular flow; frequency shift; chromatographic NMR; rheology.**

INTRODUCTION

TCDs (*t*oroid *c*avity *d*etectors, Fig. 1) have become well-established NMR resonators for insitu high-pressure NMR spectroscopy and rotating-frame NMR microscopy (*1, 2*). In both applications, they exhibit major advantages over other, more conventional NMR resonators. For example, the cylindrical geometry of TCDs and the confinement of the radiofrequency magnetic field (B_1) to within the resonator are especially suited for, and easily incorporated into, high-pressure autoclaves (*3*). In addition, TCDs exhibit radially nonuniform, mathematically well-defined B_1 fields (*3*) for one-dimensional rotating-frame microscopy and diffusiometry (*4–7*). In the vicinity of the central conductor, the B_1 gradient is sufficiently strong to provide for spatial resolutions down to the micrometer scale (*4*) even when standard spectrometer equipment is used (e.g., H band, 50 W; X band, 300 W).

In contrast to the spectroscopic and microscopic applications referenced above, we now present an NMR technique that facilitates measurement of angular (i.e., tangential) flow in TCDs. The method is based upon directional changes in the local rotating frame of reference, which nuclei experience when migrating about the central conductor. In an earlier approach, Kimmich *et al.* (*9*) have suggested flow measurements in B_1 field gradients, which utilize differences in the B_1 magnitude rather than changes in the direction of the B_1 field to discriminate between flow velocities. Accordingly, Kimmich's approach would determine radial flow rather than angular flow if applied to TCDs.

PHASE OF MAGNETIZATION IN TCDs

It has been shown and extensively exploited before (*1–6*) that the magnitude of the B_1 field in cylindrical TCDs follows precisely the simple mathematical description

$$B_1 = \frac{A}{r}, \qquad [1]$$

where A is the torus factor, i.e., the proportionality between the B_1 field and the inverse of the radial distance r (*8*). For a complete description, however, it must also be considered that the B_1 field in TCDs runs concentrically about the central conductor with the direction of B_1 continuously changing when traveling along magnetic lines of force (Fig. 1). Accordingly, the properties of the B_1 field are fully described by a vector field

$$\mathbf{B_1} = \begin{pmatrix} -\frac{A}{r}\sin(\varphi) \\ \frac{A}{r}\cos(\varphi) \\ 0 \end{pmatrix}, \qquad [2]$$

with the phase $\varphi = \omega t + \varphi_0 + \alpha$, where ω is the radiofrequency, φ_0 is the reference phase, and α is the azimuthal angle in a cylindrical coordinate system (α, r, z) in which the z axis coincides with the long axis of the TCD's central conductor. In both Eqs. [1] and [2], a dependency of the B_1 field on the z axis of the TCD is neglected (i.e., A is independent of z). This dependency was discussed before (*10*) based on the assumption that TCDs are capacitively foreshortened coaxial resonators in which standing waves (or fractions thereof) occur. However, the dependency was

[1] To whom correspondence should be addressed.

1090-7807/01 $35.00

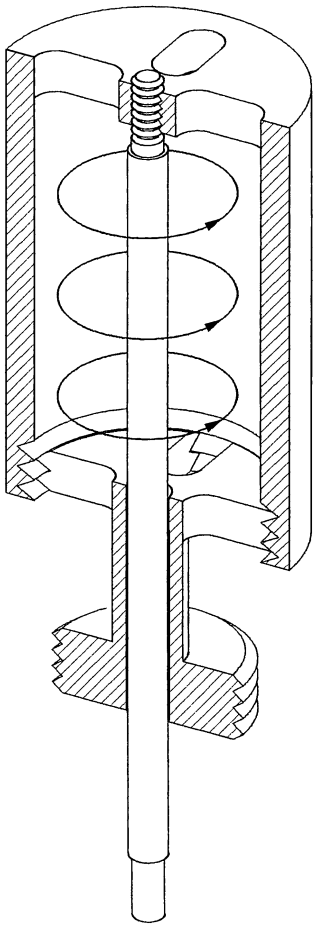

FIG. 1. Schematic drawing of a typical toroid cavity detector. The magnetic field lines are confined to the inside of the detector and lead concentrically about the central conductor.

not verified experimentally and, in addition, would not influence the results of the method presented here.

For any point inside a TCD, Eq. [2] can be used to determine the vector that fully describes the local B_1 field, i.e., revealing both the magnitude and the direction. Because radiofrequency pulses flip magnetization with a nutation frequency that depends on the B_1 magnitude and, in addition, with a phase that depends on the B_1 direction, only B_1 fields that are homogeneous in magnitude and direction achieve common flip angles and, simultaneously, common phases throughout a sample. In the center volume of a Helmholtz coil, for example, B_1 is reasonably homogeneous, so that a radiofrequency pulse (i.e., the 90° pulse) that flips the z magnetization phase-correlated into the xy plane may be determined (Fig. 2). If the sample tube is spun, angular flow occurs about the center axis of the tube but it will not change the phase of the magnetization with respect to B_1. Therefore, if the transmitter coil is also used as the receiver coil, resonances with a common phase and independent of the sample tube's angular velocity are detected. Spinning sidebands that sometimes occur when a sample tube is rotated are neglected in this discussion, because they are not based on B_1 field effects but on homogeneity deficiencies of the main magnetic field (B_0).

In TCDs, however, the B_1 field and, accordingly, the local frame of reference depends upon the phase α of Eq. [2]. Thus, a single radiofrequency pulse flips magnetization at different angular positions into different directions. For example, a single pulse during which the magnetization at a distinct radius is rotated by 90° into positions pointing radially away from the central conductor can be envisioned (Fig. 3a). If magnetization that has been fanned out in this way precesses at the transmitter frequency (i.e., on resonance), its phase remains constant with respect to the local rotating frame, and its magnitude relaxes with the time constant T_2. If, however, macroscopic angular flow occurs about the central conductor, a phase shift between the magnetization and the local rotating frame is observed (Fig. 3b). This phase shift is opposite to the direction of the imposed angular transport, so that the 45° counterclockwise sample rotation shown in Fig. 3b induces a 45° clockwise phase shift with respect to the local B_1 field. Similarly, a 90° counterclockwise sample rotation (Fig. 3c) induces a 90° clockwise phase shift. If

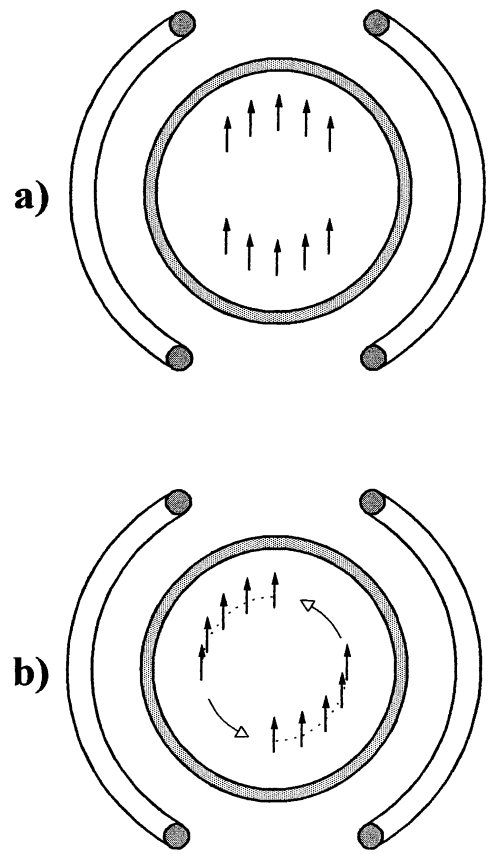

FIG. 2. Schematic drawings of a horizontal cross section through a sample tube within the sensitive area of a Helmholtz saddle coil. (a) After a 90° radiofrequency pulse, transverse magnetizations at different locations are aligned parallel. (b) If the sample tube is spun (clockwise or counterclockwise), the magnetizations change position but retain their phase with the homogeneous B_1 field of the coil.

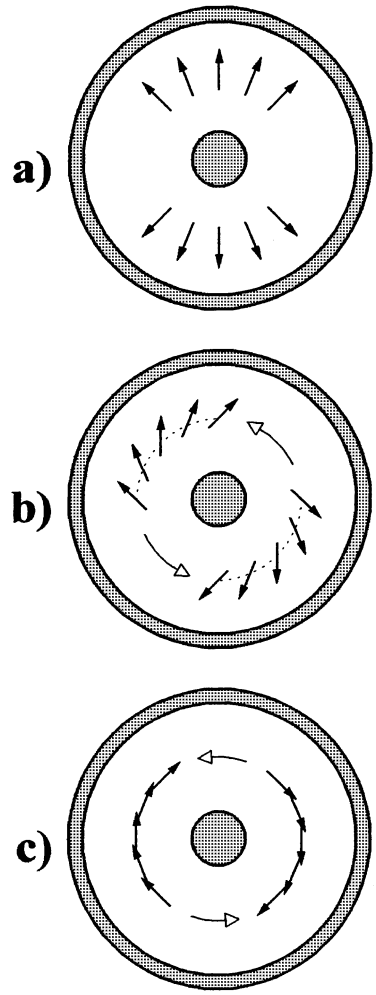

FIG. 3. Schematic drawings of a horizontal cross section through a TCD. (a) After a 90° radiofrequency pulse, transverse magnetization is fanned out, e.g., pointing away radially from the central conductor. If the sample is rotated counterclockwise, e.g., (b) by 45° or (c) by 90°, the magnetization changes angular position and phase with respect to the local B_1 field.

the magnetization precesses off resonance, macroscopic angular transport again shifts the phase with respect to the local B_1; however, this phase shift occurs in addition to the continuous phase shift (i.e., frequency shift) caused by the off-resonance precession.

The effects of magnetization transport in directional inhomogeneous B_1 fields and the accompanying phase shifts have been discussed earlier by Goldman *et al.* (*11*). In addition, frequency shifts were predicted in NMR spectra, if the direction of the B_1 field changes uniformly and continuously with the acquisition of the FID (*f*ree *i*nduction *d*ecay). Goldman *et al*. obtained these frequency shifts experimentally from sample rotation in the directional inhomogeneous fringe field of a single-loop coil. For optimum observation, the coil's center B_1 field was aligned parallel with the main magnetic field.

ROTATION INDUCED FREQUENCY SHIFTS IN TCDs

In TCDs, a continuous phase shift of transverse magnetization with respect to the local B_1 is achieved, if a sample is continuously rotated about the central conductor. Accordingly, frequency shifts similar to those predicted for other coil geometries by Goldman *et al.* are expected, if the sample is rotated with constant angular velocity. We have achieved this sample rotation with a liquid that was pumped through a capillary tube with a constant flow rate. The capillary tube was wound tightly about the TCD's central conductor in a helical fashion. Figure 4 exemplifies the geometric parameters (R, r_t, and d_t) of this capillary helix. The expected frequency shift, $\Delta\nu$, that is based on the continuous change of the local rotating frame of reference is determined from the average angular flow velocity through the capillary. This velocity is proportional to the flow rate V/t, where V is the liquid volume, and t is the time. Taking into account that a 360° sample rotation through the helix in Fig. 4 not only covers the circumference $2\pi R$ but also the height d_t, the flow rate V/t and the geometric parameters of Fig. 4 lead to

$$\Delta\nu = -\left(\frac{1}{\pi r_t^2\sqrt{(2\pi R)^2 + d_t^2}}\right)\frac{V}{t}. \qquad [3]$$

Equation [3] is based on the assumption that a positive sample rotation leads to a negative frequency shift and vice versa. If the capillary diameter, d_t, is negligibly small compared with the circumference, $2\pi R$, Eq. [3] simplifies to

$$\Delta\nu = -\left(\frac{1}{2\pi^2 r_t^2 R}\right)\frac{V}{t}. \qquad [4]$$

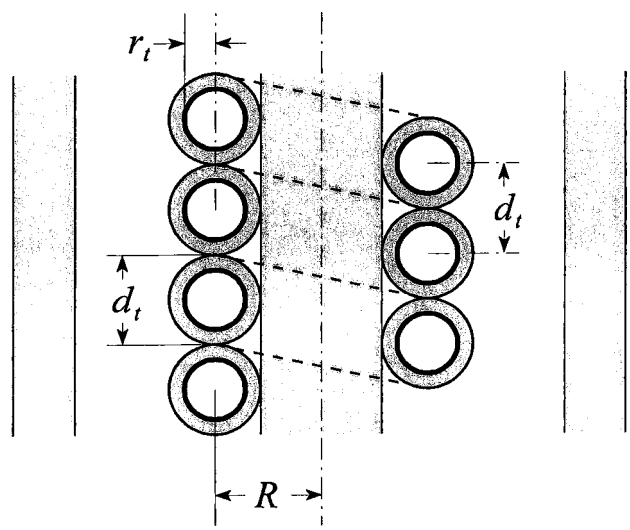

FIG. 4. Schematic drawing useful to define the geometric parameters of a capillary helix wound tightly about the central conductor of a TCD. r_t, inner capillary radius; d_t, outer capillary diameter; R, radial distance from the TCD's long axis to the capillary center.

Laminar flow in capillaries, however, is characterized by a parabolic velocity profile. Accordingly, frequency shifts calculated from Eq. [4] are volumetric mean values of a parabolic frequency-shift distribution. As a result, inhomogeneous broadening is expected for resonance lines that are shifted because of the capillary flow. In contrast, Taylor dispersion (i.e., streamline crossing because of diffusion perpendicular to the direction of flow) is expected to compensate for the line broadening to some extent.

Small frequency shifts are usually hard to determine in NMR spectra recorded without a reference signal. Especially, quantitative evaluation of the shifts is often obstructed by field drifts that might occur during or between transient measurements. In contrast, clearly visible and easy to analyze frequency shifts are achieved in NMR spectra if only one part of a resonance signal is shifted while the other one remains at its original position. Then, the frequency shift is quantified from the difference between two signals of the same spectrum. Even more pronounced is the effect of signal splitting if one part of the signal shifts into one direction (e.g., $+\Delta\nu$) while the other part is shifted by the same amount into the opposite direction ($-\Delta\nu$). Comparable to the analysis of J couplings, the shift is now determined from half the frequency difference between two signals ($J = 2\Delta\nu$). To obtain frequency shifts of equal magnitude in the positive and negative directions in our TCD flow experiment, we wound the capillary tube about the central conductor in a bifilar fashion (Fig. 5), i.e., in a double helix. At the lower end of the helix, the tube was threaded through the central conductor. During an experiment, equal amounts of sample now flow clockwise and counterclockwise through the capillary double helix. For precise evaluation of angular flow velocity (Eqs. [3] and [4]) in the double helix experiment, it must be taken into account that the height covered by one 360° sample rotation is now twice the capillary tube diameter ($2d_t$), and Eq. [3] must be amended accordingly.

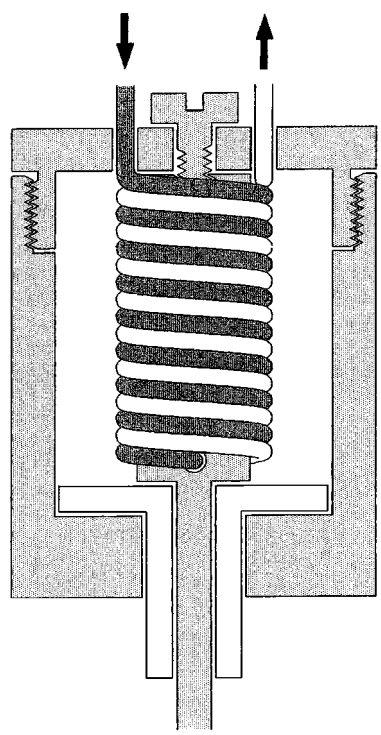

FIG. 5. Schematic drawing of a capillary helix bifilar-wound about the central conductor of a TCD.

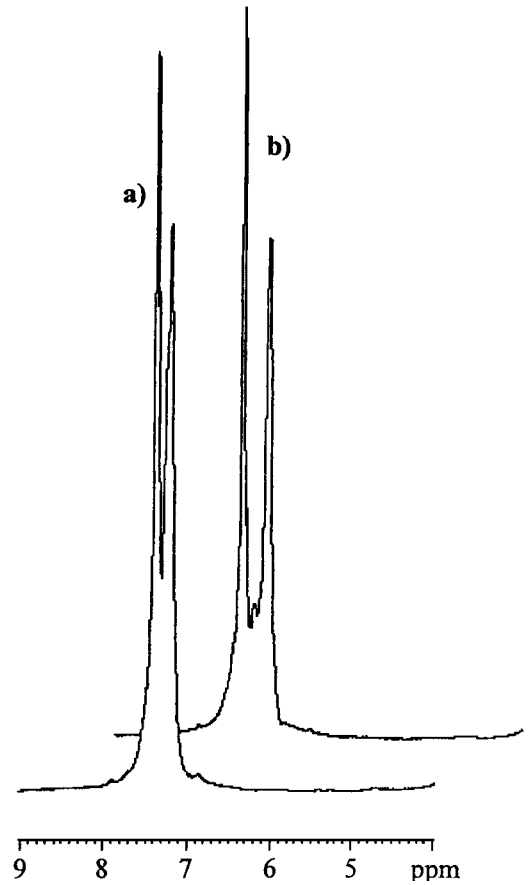

FIG. 6. ^{1}H NMR spectra of $CHCl_3$ flowing through a bifilar-wound capillary helix (Fig. 5) with different flow velocities. The signal splitting of the resonance signal of $CHCl_3$ (7.28 ppm) is the result of equal frequency shifts in the positive and in the negative directions because of clockwise and counterclockwise flow through the capillary helix. (a) $V/t = 8.00$ ml min^{-1}, $J = 33.2$ Hz. (b) $V/t = 16.00$ ml min^{-1}, $J = 64.1$ Hz.

Figure 6 shows ^{1}H NMR spectra of chloroform obtained with two different flow rates through the bifilar helix. The typical ^{1}H chloroform singlet (7.28 ppm) obtained with conventional NMR is split into two signals in the flow TCD spectra. The frequency difference between the split signals depends upon the flow velocity and precisely follows twice the amount predicted by Eq. [4]. The highly constant flow rate that was necessary to obtain the spectra of Fig. 6 was achieved with an HPLC (*h*igh-*p*erformance *l*iquid *c*hromatography) syringe pump (100 DM, ISCO Inc., Lincoln, Nebraska). The precision of Eq. [4] achieved with the chloroform experiment is depicted in Fig. 7 in which the

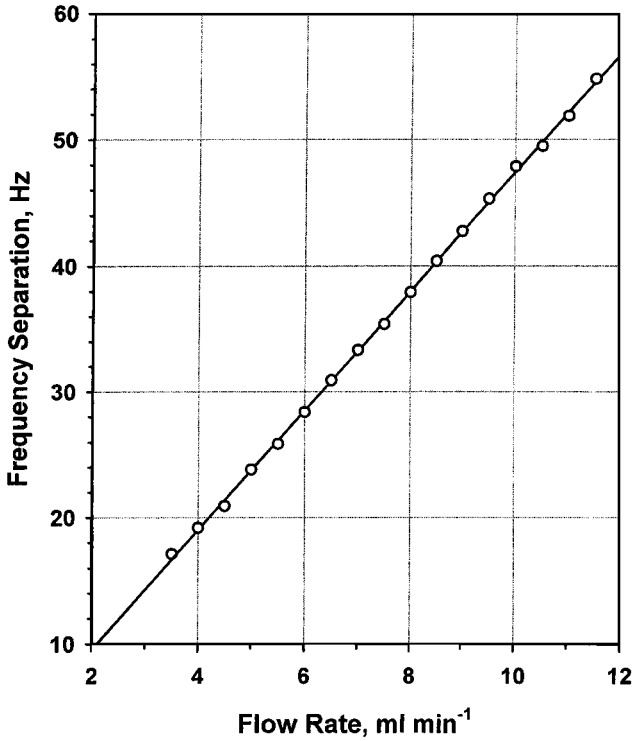

FIG. 7. Plot of frequency splitting as a function of macroscopic flow rate through the bifilar capillary helix. Experimental data (circles) are compared to the best-fit linear regression (straight line) and show the accuracy of angular flow determination.

frequency shift from different flow experiments is plotted as a function of flow rate. The data fall on a straight line with a standard deviation of less than $\pm 0.65\%$.

The chloroform was pumped with the HPLC pump that was located outside the NMR magnet. For the detection of reasonably strong signals, however, Boltzmann equilibrium at high magnetic field must be reached before the acquisition of the FID. Because relaxation to Boltzmann equilibrium takes about five times the longitudinal relaxation time, T_1, a premagnetization reservoir of about 20 ml was mounted within the flow path inside the probe right before the liquid entered the capillary-tube double helix. This reservoir provided equilibrated magnetization even for the high flow velocities.

APPLICATION TO CHROMATOGRAPHIC NMR

Samples under investigation often consist of components that must be separated before an effective spectroscopic analysis is conducted. Accordingly, chromatographic methods, such as LC (*l*iquid *c*hromatography) or HPLC, which usually precede the spectroscopic analysis, have been developed. As an alternative approach, we now propose a simultaneous, combined chromatographic and analytical technique based on the quantitative measurement of angular flow in TCDs. Instead of the capillary tube shown in Fig. 4, a chromatographic capillary is

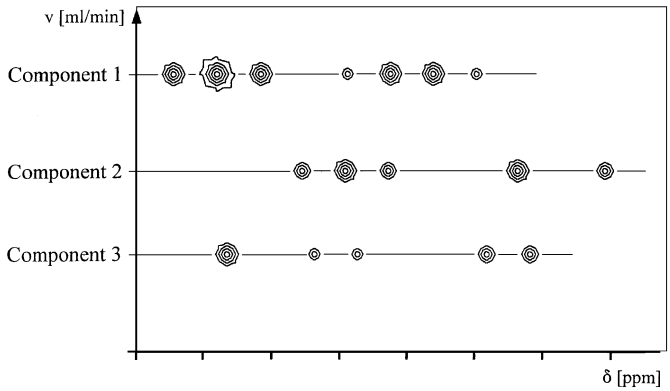

FIG. 8. Hypothetical two-dimensional spectrum as expected from chromatographic NMR. While chemical shift information (δ) is exhibited horizontally, different components (1, 2, and 3) are identified by their different flow velocities (v) resolved vertically.

wound about the central conductor, in which the angular flow velocities are different for the individual components. Consequently, different frequency shifts, which can be used for in situ discrimination between components, are expected. In an unknown mixture, however, the analysis of frequency shifts is obstructed with the analysis of chemical shifts. Therefore, a two-dimensional flow-resolved technique in which one dimension exhibits chemical shift information and the second dimension frequency shifts from angular flow is required (Fig. 8). Figure 9 shows the pulse sequence for such an NMR experiment adapted from heteronuclear *J*-resolved spectroscopy (*12*). It consists of multiple spin-echo transients in which the evolution periods τ are incrementally increased. In addition, the sequence is synchronized with the flow through the capillary. While, in heteronuclear *J* spectroscopy, *J* coupling is suppressed during the second evolution period by *turning on* a decoupler unit, the frequency shift from angular flow must be eliminated during this period by *turning off* the flow. Although it is not trivial to interrupt macroscopic flow within a very short time and without shock waves, flow-resolved NMR spectra were obtained from the flow through the bifilar helix (Fig. 5) by using a magnetic valve that was incorporated into the capillary pathway before the solution enters the TCD. The valve was positioned

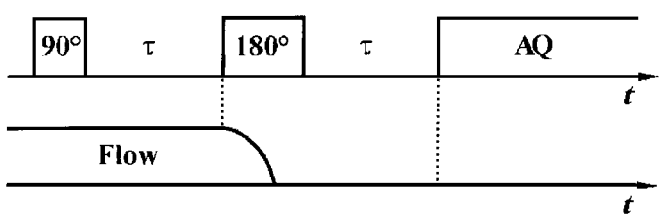

FIG. 9. Pulse sequence for resolving angular flow velocities in two-dimensional flow NMR. To obtain flow-resolved spectra, the evolution periods τ are incrementally increased and utilized for the 2D Fourier transformation (AQ, acquisition time).

underneath the superconducting magnet for its magnetic stray field must not interfere with the NMR measurement. A spare TTL connection from the NMR spectrometer's pulse sequence controller was used to gate the valve during the pulse sequence. In addition, the valve was selected shut when its electromagnet is turned off, since suppression of flow is faster this way than vice versa. Figure 10 shows the two-dimensional flow-resolved spectrum of chloroform flowing through the bifilar helix. In the chemical shift dimension, the ^{1}H chloroform signal is found at 7.28 ppm, while the second dimension reveals the clockwise and counterclockwise flow about the central conductor with angular velocities of $+21$ and -21 Hz, respectively. The signals are clearly resolved and demonstrate the capability of the proposed 2D NMR technique. Further experiments are currently under way with chromatographic capillaries.

APPLICATION TO RHEOLOGIC NMR

The capillary-tube helices of the experimental setups in Fig. 4 and Fig. 5 were assembled to measure a narrow range of radial distance within the TCD. Accordingly, pulse sequences exhibit a reasonably uniform flip angle even in the TCD's strongly inhomogeneous B_1 field. Alternatively, however, the B_1 gradient can be utilized for one-dimensional RFM (*r*otating *f*rame *m*icroscopy) (*4*). Hence, angular flow caused by sample rotation (i.e., rotation-induced frequency shifts) can also be resolved as a function of radial position. TCD microscopic techniques in which flow properties are resolved as a function of spatial dimension will be termed rheologic RFM. A possible setup for rheologic RFM is shown in Fig. 11 where the central conductor of a TCD is rotated versus the outer cylinder. Alternatively, the central conductor could be fixed while the outer body is spun. The velocity profiles that occur when either the central conductor or the outer body is spun can be imaged with standard RFM (*4*). Based on the rheologic RFM concept, the construction of a rheologic TCD probe with rotating central conductor is currently under way.

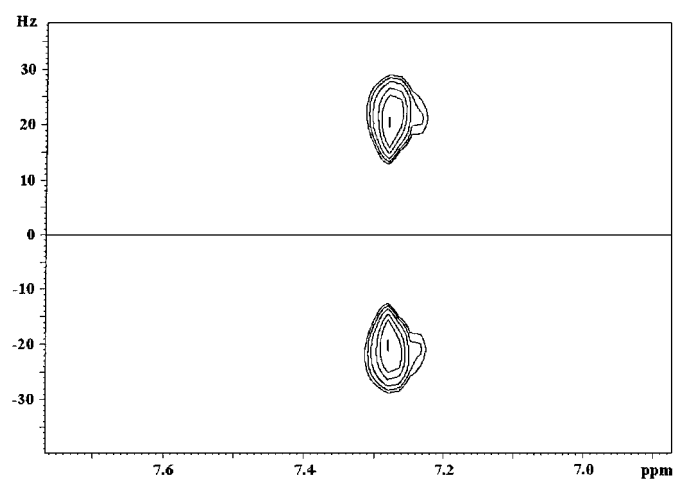

FIG. 10. Two-dimensional ^{1}H flow-resolved NMR spectrum obtained from chloroform flowing through the capillary helix bifilar-wound about the central conductor (Fig. 5). The signal at $\delta = 7.28$ ppm (chemical shift axis) is split into the two clearly resolved resonances of opposite flow ($+21$ and -21 Hz, velocity axis).

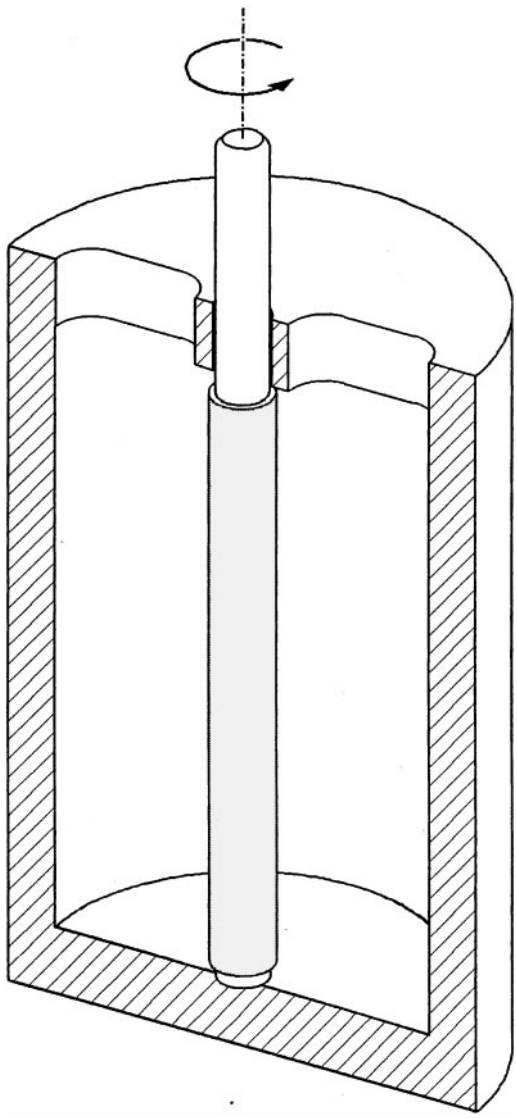

FIG. 11. Schematic drawing of a TCD for rheologic studies. If the central conductor is spun versus the outer hollow body (or vice versa), a radially dependent angular velocity profile occurs within the sample area of the TCD. With rheologic RFM, this profile is resolved as a function of radial distance.

CONCLUSION

A new NMR spectroscopic technique that greatly expands the field of applications for TCDs is presented. It is found that sample rotation in the directionally inhomogeneous B_1 field of TCDs leads to frequency shifts of NMR signals, which correspond to the negative angular velocity of sample components. The effect is explained by a continuous phase shift (i.e.,

rotation) of the local rotating frame of reference, which occurs for volume elements that travel along a B_1 field line. Accordingly, the observation of frequency shifts is effectively connected with the B_1 field lines of TCDs leading concentrically about the central conductor. While these frequency shifts must be carefully considered if sample rotation is applied as an NMR spectroscopic tool to TCDs, e.g., in MAS (*m*agic-*a*ngle *s*pinning) for line narrowing in solid state NMR (*13*), they can be utilized in applications such as chromatographic or rheologic NMR.

ACKNOWLEDGMENTS

This work was supported by the German Research Foundation (DFG) under Program WO 613/2-2 and in part by the U.S. Department of Energy, Division of Chemical Sciences, Office of Basic Energy Sciences, under Contract W-31-109-Eng-38. We thank Bernd L. J. Zwank (University of Bonn) and Robert J. Klingler (Argonne National Laboratory) for stimulating discussions during the initial development of this work, and Erwin L. Hahn (University of California, Berkeley) for relating our work to the physics of the Doppler effect and the Berry phase.

REFERENCES

1. J. W. Rathke, R. J. Klingler, R. E. Gerald II, K. W. Kramarz, and K. Woelk, Toroids in NMR spectroscopy, *Prog. NMR Spectrosc.* **30,** 209–253 (1997).
2. J. W. Rathke, R. J. Klingler, R. E. Gerald II, D. E. Fremgen, K. Woelk, S. Gaemers, and C. J. Elsevier, NMR spectroscopy, *in* "Chemical Synthesis Using Supercritical Fluids" (P. G. Jessop and W. Leitner, Eds.), pp. 165–194, Wiley–VCH, Weinheim (1999).
3. K. Woelk, J. W. Rathke, and R. J. Klingler, The toroid cavity NMR detector, *J. Magn. Reson. A* **109,** 137–146 (1994).
4. K. Woelk, J. W. Rathke, and R. J. Klingler, Rotating-frame NMR microscopy using toroid cavity detectors, *J. Magn. Reson. A* **105,** 113–116 (1993).
5. K. Woelk, R. E. Gerald II, R. J. Klingler, and J. W. Rathke, Imaging diffusion in toroid cavity probes, *J. Magn. Reson. A* **121,** 74–77 (1996).
6. K. Woelk, B. L. J. Zwank, J. Bargon, R. J. Klingler, R. E. Gerald II, and J. W. Rathke, Imaging diffusion with nonuniform B_1 gradients, *in* "Spatially Resolved Magnetic Resonance" (P. Blümler, B. Blümich, R. Botto, and E. Fukushima, Eds.), pp. 103–110, Wiley–VCH, Weinheim, 1998.
7. K. Woelk, B. L. J. Zwank, P. Trautner, E. Lehnhof, J. Bargon, R. J. Klingler, R. E. Gerald II, and J. W. Rathke, High-precision diffusion measurement through finite-difference evaluation of rotating-frame images, *J. Magn. Reson.* **145,** 276–290 (2000).
8. K. Woelk, Torus factor—The relationship between radiofrequency field and radial position in toroid cavity probes, *J. Magn. Reson.* **146,** 157–164 (2000).
9. R. Kimmich, B. Simon, and H. Köstler, Magnetization-grid rotating-frame imaging technique for diffusion and flow measurements, *J. Magn. Reson. A* **112,** 7–12 (1995).
10. G. A. Barrall, Y. K. Lee, and G. C. Chingas, Radial RF imaging using a coaxial resonator, *J. Magn. Reson. A* **106,** 132–134 (1994).
11. M. Goldman, V. Fleury, and M. Guéron, NMR frequency shift under sample spinning, *J. Magn. Reson. A* **118,** 11–20 (1996).
12. R. Freeman, "A Handbook of Nuclear Magnetic Resonance," pp. 106–110, Longmans Scientific & Technical, Essex, UK (1988).
13. R. E. Gerald II, R. J. Klingler, and J. W. Rathke, Disclosure of the rotational exchange gradient imager, poster presentation at the 42th Rocky Mountain Conference on Analytical Chemistry, Broomfield, CO, July 30–August 3, 2000.